ENTROPY PRODUCTION AND COLLECTIVE PHENOMENA IN BIOLOGICAL CHANNEL GATING

Bartosz Lisowski[a,b,†], Michał Żabicki[a], Bartłomiej Dybiec[a]
Ewa Gudowska-Nowak[a]

[a]M. Smoluchowski Institute of Physics
and M. Kac Complex Systems Research Center, Jagiellonian University
S. Łojasiewicza 11, 30-348 Kraków, Poland
[b]Unit of Pharmacoepidemiology and Pharmacoeconomics, Faculty of Pharmacy
Jagiellonian University Medical College, Medyczna 9, 30-688 Kraków, Poland

(Received February 12, 2019; accepted March 11, 2019)

We investigate gating kinetics of biological channels influenced by conformational changes within the membrane proteins forming the module, and subject to a coupling with other similar units. By introducing elements of stochastic thermodynamics, we analyze the information flow and associated entropy production during gating cycle of a single channel. In the second part of this paper, synchronized kinetics of multiple units of that type is analyzed in terms of Kuramoto's theory.

DOI:10.5506/APhysPolB.50.911

1. Introduction

Inorganic compounds are necessary for life. They provide building blocks for biomolecules, *e.g.* enzymes, chlorophyll or hemoglobin and act as signaling agents and osmotic pressure determinants, to name only few of their multiple functions. However, living cells cannot synthesize inorganic ions. They have to absorb them from the surrounding. This is a serious challenge, requiring continuous monitoring and regulation of ions concentrations. This regulation — moving the ions from and to the environment, according to the physiological needs of an organism — is possible due to the action of ion channels.

Ion channels are specialized proteins which, together with ion pumps, sort the charges on both sides of the plasma and/or organelle membranes. They are found in all mammalian cells and their physiological roles range

† Corresponding author: bartek.lisowski@uj.edu.pl

from bulk ion transport to subtle electrogenic signaling. Many ion channels are closed most of the time, but open in response to specific physiological stimuli, such as altered concentration of specific compounds, membrane potential changes, or temperature shifts [1]. Particularly, the voltage-gated ion channels are involved in plethora of physiological processes and form pertinent building blocks of signal transduction and processing at different levels of multicellular organization [2, 3]. The flow of ions across a membrane implies a transmembrane electrical current. Though the electrical current through an individual channel is of picoampere magnitude, it can be followed in certain experimental setups [1–6].

Ion channels, like all proteins, are generally very polar molecules and the open-closed transitions usually involve significant movement of charge. The energetics associated with charge movement change when the transmembrane potential changes. It is thus that the ion currents that are caused by channel opening can have a feedback on the open–closed kinetics itself. It is a positive feedback of this kind that produces the propagation of a signal through a nerve cell [1].

The aforementioned feedback can also lead to memory effects in the behavior of clusters of ion channels. In response to a varying external stimulus (*e.g.* applied voltage or temperature), clusters of ion channels have actually been observed to exhibit hysteresis [4–13]. Hysteresis is a mechanism commonly exploited in data storage and synthetic memory applications [5, 13]. It is still a question to what extent hysteretic gating of biological channels is involved in the storage and transmission of information at molecular level [7, 14, 15].

In this article, we use a formerly proposed simple channel gating model [9, 12]. This model exhibits a lagged response to external forcing. With the methods of stochastic thermodynamics [7, 14–21], we explore energy flows associated with channel gating and we describe how conformationally coupled ion channels synchronize their open–closed kinetics. Furthermore, to quantify the signal transduction encoded in current traces and to analyze the transmission of information associated with the conformational changes of the channels, we introduce a formal analysis based on Shannon's definition of entropy.

2. Model of a single channel kinetics

To describe gating mechanism of a single ion channel, we use a 4-state model, introduced in [9, 12], see Fig. 1. The scheme represents opening and closing kinetics of a non-selective ion channel, which is activated at depolarizing potentials and has been shown [6] to exhibit counter-clockwise gating hysteresis. The simple Boltzmann statistics can be used to fully reproduce

kinetics of the gating, including direction of the hysteresis cycle [9, 12] by assuming 2×2 discrete states: the normal open/closed states and two different states of "gate tension". Accordingly, (σ_c, σ_g) are binary variables — $\sigma_c = \pm 1$, $\sigma_g = \pm 1$ — denoting states of an open/closed channel and configurational changes within the channel gate, respectively. The membrane protein changes its conformation in a series of intermediate steps [9, 22, 23] causing the open-probability of the channel's gate to depend on the actual state of the protein. To acknowledge those additional internal degrees of freedom (σ_c), two transient states (semi-open $\mathbf{2} = (-1, 1)$ and semi-closed $\mathbf{4} = (1, -1)$) are introduced. Pulling the part of the protein which forms the gate by external forces (*e.g.* voltage) results in reaction of attached parts of the membrane to this pull. If the protein has two different conformational states, it can yield to this pull and change to a state of a lower energy for the given state of the gate.

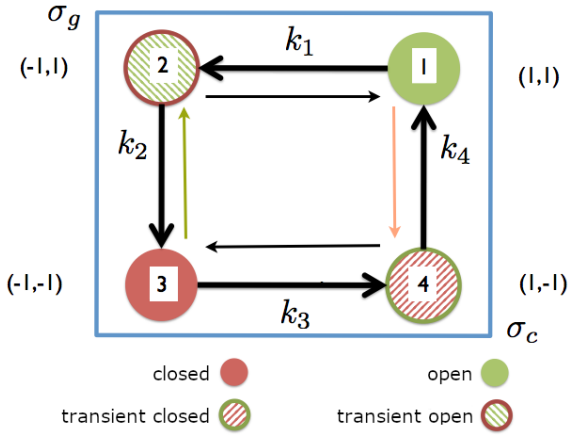

Fig. 1. The four-state model of channel gating parametrized by discrete variables representative for a gate and a given conformation state (σ_g, σ_c). The upper two states have an open gate and the lower two, closed. The states to the right favor open gate whereas the ones to the left, closed. Vertical transitions are those between open and closed gate, while parallel describe transitions between configurational states of the channel protein which favor open/closed gates.

The model can be easily generalized by replacing two states of different gate tension by a real value, collective coordinate $\bar{x}$ which stands for a conformational change within the gate [9]. Within this scheme, the reaction pathway of this change is defined in terms of a corresponding potential $W(\bar{x})$ describing the protein's internal energy as a function of the coordinate $\bar{x}$. Since the gate's thermally driven changes between its open and closed state are assumed to take place much faster than the protein's changes of gate

tension, the latter, parametrized by $\bar{x}$, take place in the effective potential $W_{\mathrm{eff}}(\bar{x}; V_{\mathrm{m}})$ that results from summing over both states of the gate,

$$\begin{aligned} e^{-W_{\mathrm{eff}}(\bar{x};V_{\mathrm{m}})} &= p(\bar{x}) \\ &= \sum_{\sigma_{\mathrm{g}}=\pm 1} p(\sigma_{\mathrm{g}}, \bar{x}) \propto \sum_{\sigma_{\mathrm{g}}=\pm 1} e^{-E(\sigma_{\mathrm{g}},\bar{x})} \\ &= e^{-E_0 - W(\bar{x})}\, 2\cosh\left(\tfrac{1}{2}\Delta E_{\mathrm{g}}(V_{\mathrm{m}}) + \tfrac{1}{2}\Delta E_{\mathrm{i}}\,\bar{x}\right) . \end{aligned} \tag{2.1}$$

Here, $E(\sigma_{\mathrm{g}}, \bar{x}) = E_0 + \frac{1}{2}\Delta E_{\mathrm{g}}(V)\,\sigma_{\mathrm{g}} + W(\bar{x}) + \frac{1}{2}\Delta E_{\mathrm{i}}\,\sigma_{\mathrm{g}}\bar{x}$ is the internal energy of the system defined up to a constant E_0, $\Delta E_{\mathrm{g}}(V_{\mathrm{m}})$ describes energy contribution from the gate, ΔE_{i} describes the energy of interaction between the gate and the protein, and V_{m} stands for the membrane potential. Such parametrization results in a two-dimensional structure of an effective potential as displayed in Fig. 2. Rates of transitions between the two branches of the observed hysteresis curve can be then modeled with the single-barrier Kramers kinetics. When described in terms of the effective potential with cyclic variations of the control parameter (an activating voltage), such a system has been shown to exhibit typical noise-controlled "resonant effects": synchronization, resonant activation and stochastic resonance [10–12]. As discussed in [9, 12], occurrence of the phenomena can be investigated by simulating stochastic dynamics (*cf.* Fig. 3) of the model and performing statistical analysis of gating trajectories.

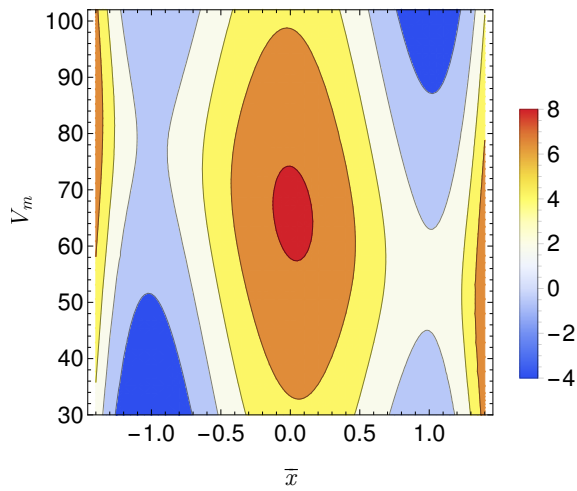

Fig. 2. (Color online) The effective potential $W_{\mathrm{eff}}(\bar{x}; V_{\mathrm{m}})$ (marked in colors) for the four-state model of channel gating described in the text. The most stable open/closed states are depicted in the upper right/lower left corners of the plot, respectively.

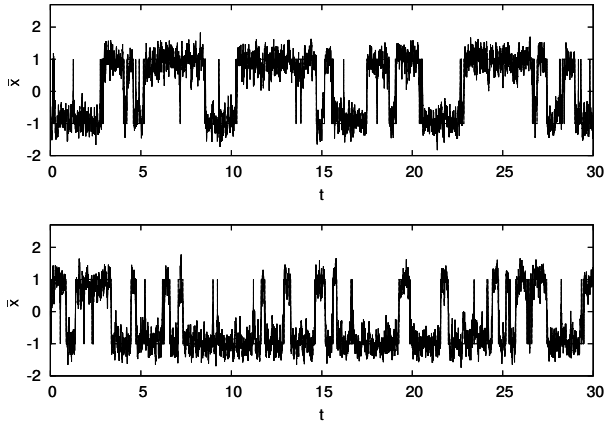

Fig. 3. A long trajectory of the effective "reaction coordinate" derived from the four-state model. Transition events are modeled by the use of the prototypical Langevin equation, *i.e.* as a passage of a test particle moving in the potential well $W_{\mathrm{eff}}(\bar{x}; V_{\mathrm{m}})$ and driven by fluctuating solvent (environment) represented by action of random Gaussian forces.

3. Cell membrane as a carrier of bio-information

In line with Shannon's concepts of signal processing, we will use the relation between information acquisition and entropy production, originating from Schrödinger [13, 24] and, more recently, reintroduced in analysis of nanoscale systems by stochastic thermodynamics [16, 18–21]. Stochastic thermodynamics extends classical thermodynamics to small systems in contact with environment (heat bath). The main idea is that state functions (like entropy itself) can be expressed by the same relations as in the standard irreversible thermodynamics, except of the fact that now, the state variables are random variables, and their evolution accounts for fluctuations influencing the system beyond equilibrium state. It has been previously shown how the thermodynamic response of ion channels becomes affected by abrupt perturbations of the system, for example, with an external voltage [13–15]. Below, we analyze consequences of channel response to additional tension on the gate causing either its stiffening or loosening, thus favoring or disfavoring its opening. For this purpose, we extend former analysis of the model from [9, 12] by looking at the single ion channel as an information conductor. The additional degrees of freedom, *i.e.* states 2 and 4 in Fig. 1, account for the channel's complex dynamics. Before the fast opening/closing transitions, the protein changes its conformation in a series of slow steps, symbolized here by the two transient states. This separation of fast and slow processes allows to treat the channel as a bipartite system [17, 19]. For such a system, a detailed knowledge about the entropy production and information flow may be obtained [19–21].

Following derivations presented in [20, 21], we extend the original model by describing channel gating kinetics (Fig. 1) in terms of a Markovian bipartite system whose time-dependent joint probability distribution $p(\sigma_c, \sigma_g; t) \equiv p(x, y; t)$ evolves according to a master equation:

$$\frac{\mathrm{d}}{\mathrm{d}t}p(x,y;t) = \sum_{x',y'} \left[K^{y,y'}_{x,x'} p\left(x',y';t\right) - K^{y',y}_{x',x} p(x,y;t) \right] . \tag{3.1}$$

The transition matrix $K^{y,y'}_{x,x'}$ for a transition from (x', y') to (x, y) is of the form of

$$K^{y,y'}_{x,x'} = \begin{cases} k^{y}_{x,x'}\Delta t & \text{for} \quad x \neq x' \quad \text{and} \quad y = y' \\ k^{y,y'}_{x}\Delta t & \text{for} \quad x = x' \quad \text{and} \quad y \neq y' \\ 0 & \text{otherwise,} \end{cases} \tag{3.2}$$

and satisfies the normalization condition $\sum_{x,y} K^{y,y'}_{x,x'} = 1$. Accordingly, the states parametrized by x and y influence each other but never change simultaneously.

The master equation can be also recast in the form of a continuity equation with currents $J^{y}_{x,x'} \equiv k^{y}_{x,x'} p(x', y; t) - k^{y}_{x',x} p(x, y; t)$ and $J^{y,y'}_{x} \equiv k^{y,y'}_{x} p(x, y'; t) - k^{y',y}_{x} p(x, y; t)$. Equation (3.1) then reads

$$\frac{\mathrm{d}}{\mathrm{d}t}p(x,y;t) = \sum_{x',y'} J^{y,y'}_{x,x'} = \sum_{x'} J^{y}_{x,x'} + \sum_{y'} J^{y,y'}_{x} . \tag{3.3}$$

Entropy production rate $\dot{S}_i(t)$ for the system can be easily derived [20] by analyzing time derivative of the system's Shannon entropy (with a Boltzmann constant k_B set to 1)

$$\begin{aligned} S(t) &= -\left\langle \ln p\left(\sigma_c = x, \sigma_g = y; t\right)\right\rangle , \\ \frac{\mathrm{d}S}{\mathrm{d}t} &= \dot{S}_e(t) + \dot{S}_i(t) , \end{aligned} \tag{3.4}$$

where

$$\dot{S}_i(t) = \sum_{x\neq x',y} J^{y}_{x,x'} \ln \frac{k^{y}_{x,x'} p\left(x',y;t\right)}{k^{y}_{x',x} p(x,y;t)} + \sum_{x,y\neq y'} J^{y,y'}_{x} \ln \frac{k^{y,y'}_{x} p\left(x,y';t\right)}{k^{y',y}_{x} p(x,y;t)} \geq 0 , \tag{3.5}$$

$\dot{S}_e(t)$ is the entropy flow to the environment and average in Eq. (3.4) is taken over the joint probability distribution function $p(x, y; t)$.

In line with a full kinetic scheme displayed in Fig. 1, we will refer to eight kinetic rates: $k^{+}_{-,+} \equiv k_{12}$, $k^{+}_{+,-} \equiv k_{21}$, $k^{-}_{+,-} \equiv k_{34}$, $k^{-}_{-,+} \equiv k_{43}$ which describe change of a conformation state $\sigma_{\rm c} = x$ while preserving the same state of the gate $\sigma_{\rm g} = y$ and $k^{-,+}_{-} \equiv k_{23}$, $k^{+,-}_{-} \equiv k_{32}$, $k^{-,+}_{+} \equiv k_{14}$, $k^{+,-}_{+} \equiv k_{41}$ which describe the closing and opening of the gate at a constant conformation state. Note, that according to the notation in Eqs. (3.1), (3.2), upper indices refer to the sign of the gate binary variable, whereas lower ones denote the sign of $\sigma_{\rm c}$.

At equilibrium, the detailed balance condition has to be satisfied, *i.e.* $k_{12} \times k_{23} \times k_{34} \times k_{41} = k_{14} \times k_{43} \times k_{32} \times k_{21}$ yielding zero entropy change $\dot{S}(t) = 0$. In turn, in stationary nonequilibrium states, the latter condition is violated and non-zero currents contribute to nonnegative entropy production expressing energetic costs of channel gating at varying conformation state of the ion channel.

We assume that the state of a fully open channel ($\sigma_{\rm c} = 1, \sigma_{\rm g} = 1$) is the highest (excited) energetic state, separated from the lowest one ($\sigma_{\rm c} = -1, \sigma_{\rm g} = -1$) by two additional "semi-open" and "semi-closed" states of intermediate energies (*cf.* Fig. 1). Relaxation from the fully open state **1** can be realized by decay with rate a to a semi-closed state **4**, or by decay with rate b to the semi-open state **2**. The transition from state **4** to **1** requires some extra energy to be applied and can be realized with rate $ae^{-\epsilon}$. Similar reasoning explains rates between other pairs of states, listed in Table I. The explicit form of the entropy production rate associated with the steady state of the system can be written as

$$\dot{S}_i(t) = 2\left[J_{34}\ln\frac{k_{34}p(3)}{k_{43}p(4)} + J_{21}\ln\frac{k_{21}p(2)}{k_{12}p(1)} + J_{32}\ln\frac{k_{32}p(3)}{k_{23}p(2)} + J_{41}\ln\frac{k_{41}p(4)}{k_{14}p(1)}\right] \tag{3.6}$$

with $p(i)$ standing for steady-state probabilities and J_{ik} indicating steady currents between states i and j, respectively. By using as entry parameters the rates from the first column of Table I, we get steady-state probabilities $p(1) = p(2) = (2 + 2e^{\epsilon})^{-1}$ and $p(3) = p(4) = e^{\epsilon}p(1)$. Accordingly, steady state flows between any two pair of states become zero:

$$\begin{aligned} J_{12} &= J_{21} = p(1)b - p(2)b = 0\,, \\ J_{23} &= J_{32} = p(2)a - ae^{-\epsilon}p(3) = 0\,, \\ J_{41} &= J_{14} = p(1)a - ae^{-\epsilon}p(4) = 0\,, \end{aligned} \tag{3.7}$$

in line with the detailed balance condition. In other words, unperturbed, independently operating ion channel does not produce entropy during its repetitive opening and closing cycles. However, as discussed extensively in the next section, channels exhibit collective phenomena by detecting and

responding to the state of their neighbors. For example, the opening of one channel affects the opening probability of its neighbor [3]. To acknowledge this fact, we introduce the interaction term $\exp[\pm\Delta G]$ with $\Delta G \geq 0$ to some of the rates from Table I. Positive exponent, $\exp[+\Delta G]$, means that the environment (*e.g.* the other channel) favors the transition. Similarly, negative exponent, $\exp[-\Delta G]$, indicates that the system opposes to change its state. We consider two cases: the favoring of the open state, when the environment supports the transitions towards state 1, and of the closed state, with preferential transitions towards state 3. Since the experimentally obtained time series of channel's opening and closing do not distinct between the main (*i.e.* open or closed) and the indirect (*i.e.* semi-open and semi-closed) states, we modify also the rates of the transitions from and to the corresponding transients. Table I lists the corresponding sets of transition rates.

TABLE I

Transition rates during the opening and closing cycle of a single ion channel. Second column lists the rates for an independent channel, unaffected by the environment. Third and fourth columns list the rates for a channel with favored open state 1 and closed state 3, respectively.

Rate	Normal	Favoring open	Favoring closed
k_{12}	b	$b\exp[-\Delta G]$	b
k_{21}	b	$b\exp[\Delta G]$	b
k_{23}	a	$a\exp[-\Delta G]$	$a\exp[\Delta G]$
k_{32}	$a\exp[-\epsilon]$	$a\exp[-\epsilon+\Delta G]$	$a\exp[-\epsilon-\Delta G]$
k_{34}	b	b	$b\exp[-\Delta G]$
k_{43}	b	b	$b\exp[\Delta G]$
k_{41}	$a\exp[-\epsilon]$	$a\exp[-\epsilon+\Delta G]$	$a\exp[-\epsilon-\Delta G]$
k_{14}	a	$a\exp[-\Delta G]$	$a\exp[\Delta G]$

For these transition rates (3^{rd} and 4^{th} columns in Table I), we calculate the stationary probabilities and flows. With the rates affected by the environment, the detailed balance is violated and the nonvanishing currents occur in the system, driving the cycle depicted in Fig. 1 away from the equilibrium. This results in the positive entropy production rate $\dot{S}_i(t) > 0$. Figure 4 shows the entropy production rate at nonequilibrium steady states as a function of the interaction energy ΔG, when the environment supports both opening and closing of a given ion channel. When the environment favors channel opening, with increasing ΔG the system is more likely to stay in state 1. Eventually, for ΔG big enough, escape from state 1 becomes

impossible and the channel "freezes out". For a certain value $\Delta G = \Delta G_{\max}$, entropy production rate $\dot{S}_i(t)$ reaches a maximum. In this case, the system reaches nonequilibrium steady state with corresponding steady state fluxes $J_{21} = J_{32} = -J_{34} = -J_{41}$. Analogical scenario (*cf.* lower curve in Fig. 4) takes place when the closed state of the channel becomes preferred.

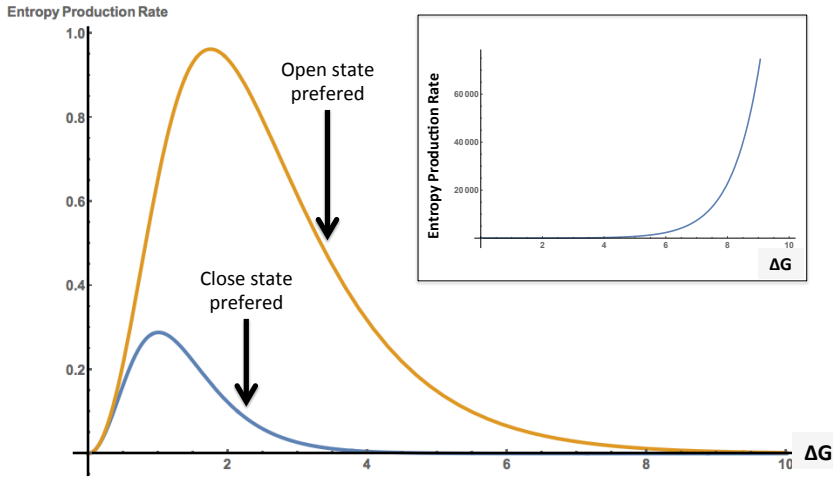

Fig. 4. (Color online) Entropy production rate $\dot{S}_i$ as a function of environmental pressure ΔG. Light gray/orange plot shows the entropy production when the interaction with the environment favors the open state of a channel. Gray/blue plot shows the same dependency for the enforced closed state. The parameter values are $a = 10$, $b = 0.1$ and $\epsilon = 1$. The inset shows the entropy production rate for an irreversible cycle $1 \to 2 \to 3 \to 4 \to 1$ as a function of ΔG. The nonequilibrium probabilities are: $p_1 = 2/4, p_2 = 1/4, p_3 = 1/8, p_4 = 1/8$.

We note that the entropy production can also be calculated for a simplified, irreversible cycle $1 \to 2 \to 3 \to 4 \to 1$ [7]. With nonequilibrium time-dependent probabilities $p(x, y; t)$, the entropy production rate grows exponentially with increasing ΔG (inset in Fig. 4) and falls to zero when the equilibrium is reached.

To acknowledge the composite nature of channel gating, we may separate the transitions responsible for opening and closing of the channel (vertical lines in Fig. 1) from the changes in its gate tension (horizontal lines in Fig. 1) [19]. It allows to compare entropy production rates by the two subsystems, *i.e.* during internal changes in the protein, leading to the global effect — gating. They are given by

$$\dot{S}_i^X = \sum_{x \neq x'; y} J^y_{x,x'} \ln \frac{w^y_{x,x'} p\,(x', y)}{w^y_{x',x} p(x, y)}\,,$$

$$\dot{S}_i^Y = \sum_{x;y\neq y'} J_x^{y,y'} \ln \frac{w_x^{y,y'} p\,(x,y')}{w_x^{y',y} p(x,y)}\,. \tag{3.8}$$

As described by Horowitz and Esposito [19], this separation can be used to write down the second law for both subsystems, X and Y. Figure 5 shows entropy production rates for both subsystems of an ion channel: global conformational changes, which lead to opening/closing, and additional "degrees of freedom" or gate tension.

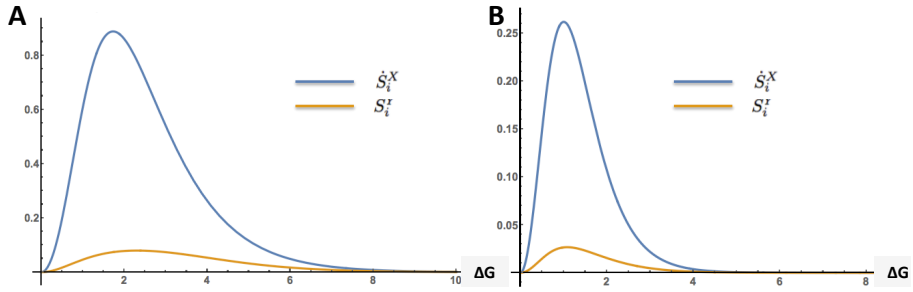

Fig. 5. Entropy production rates in two separated subsystems: opening/closing (*i.e.* "Y transitions") and gate tension (*i.e.* "X transitions") of the channel. Panel shows the entropy production rates along X and Y transitions when open (**A**) and closed (**B**) state is favored.

Untill now, we have analyzed some thermodynamical properties of a single ion channel. The only interaction with the nonspecified environment was via the constant term $\exp[\pm\Delta G]$ in the transition rates. Now, we turn towards more realistic scenario of an idealized membrane, containing multiple channels. There will be a reciprocal interaction between every channel and its neighbors. This interaction will have a serious consequences for the physiology of a whole cell.

4. Synchronization in the group of channels

In living cells, ion channels do not work independently of one another. Collective behavior has been observed in numerous experiments [25–27] and mutual cooperativity of channels has been attributed to both, internal parameters (structural variations) and external factors (membrane proteins). Notwithstanding, the underlying mechanism by which the membrane proteins "communicate" is still not obvious. One way of propagating the signal about the given channel's state is via the membrane. Open channel changes the structure of nearby lipids in a different way than does the closed one [28–30]. Hence, the membrane deformation can be a realization of a coupling,

but only on short distances. Another possibility is the change of ion gradient between both sides of the membrane. With the opening of channels, the ions start to flow from and/or inside the cell, changing the transmembrane potential V_{m}. The more open channels, the bigger the change in the electric field and the collective response of other channels. The same effect can be also achieved experimentally by applying the external potential as in [9].

Ion channel clusters, *i.e.* regions on a membrane where the action of one channel is amplified by the actions of the neighboring ones [31–35] have been found in many cell types and have been documented to play an important role in signal transduction. For example, specific targeting, clustering and maintenance of Na^+ and K^+ channels in myelinated nerve fibers are essential to achieve high conduction velocities of action potential propagation [36]. It has been also reported [37] that distributions of receptors in clusters of variable sizes optimize the response to small stimuli and the sensitivity to signal amplitudes. Similar conclusions have been drawn by Shuai and Jung [34] who, in their studies of inositol 1,4,5-triphosphate receptors in the plasma membrane, have shown that channel clustering can dramatically enhance the cell's capability of creating a large Ca^{2+} response to weak stimulation.

At the level of statistical analysis of signals, one of useful measures of channel–channel interaction is assessing the number of ion channels opening under voltage clamped conditions [38]. To study such collective behavior of channels, here we address a model system of n channel units distributed over interacting clusters. Throughout this section, for a single channel, we will use the simplified transition cycle in which all the reactions showed in Fig. 1 vary periodically, *i.e.* $1 \to 2 \to 3 \to 4 \to 1 \ldots$ The transitions between subsequent states of the channel are then reminiscent of a phase-change of an oscillator [31]. For an isolated channel, the transition rate $k_1 = k_2 + k_3 = k_4$ is now set to a constant k_0 with a system reaching a steady state $p_1 = p = 2 = p_3 = p_4 = 1/4$. For many coupled units, the transition rates are assumed to depend on the state of neighboring units (thus, coupling neighboring phases). To study emergence of synchrony in the system of interacting channels, following Wood *et al.* [31], we define the transition rate k_i of a single unit (a single four-state channel) from state i to state $i+1$ as

$$k_i = k_0 \exp\left[\frac{a\,(VN_{i-1} + UN_{i+1} + WN_i)}{n}\right], \tag{4.1}$$

where $i = 1, 2, 3, 4$ and $i + 1 = 1$ when $i = 4$ and $i - 1 = 4$ when $i = 1$. In this way, each unit is globally coupled to $n - 1 \to \infty$ units (among which N_i are in state i). U, V and W are real parameters responsible for coupling strength with units in certain states. For a given set of channels, they are determined once and for all. Parameter a, however, is a continuos variable.

It has been shown that ion channels tend to form clusters, *i.e.* such regions on a membrane where the action of one channel is amplified by the actions of the neighboring ones [32–35]. They do so under the meticulous control of the cytoskeleton and other assisting proteins [30]. In our case, the strength of the amplification is determined by the choice of parameters U, V, W. Additionally, we assume that the more channels interact, the bigger the collective effect [38]. This feature is captured in the progressive change of a. It may, or may not, grow linearly. Here, we take the simple case of $a \propto L$, with L being the cluster size, *i.e.* the number of channels in a given cluster.

We start with expressing the probability of finding, for the i^{th} unit, N_j among n units in state $j = \{i-1, i, i+i\}$ as $P_i = N_j/n$. Equation (4.1) then reads

$$k_i = k_0 \exp\left[a\left(VP_{i-1} + UP_{i+1} + WP_i\right)\right] . \tag{4.2}$$

For a set of equations

$$\dot{P}_i = k_{i-1}P_{i-1} - k_iP_i \,, \tag{4.3}$$

we calculate the stationary probabilities P_i^0, obtaining $P_i^0 = (k_{i-1}/k_i)P_{i-1}^0$. By taking $P_1^0 = P_2^0 = P_3^0 = P_4^0 = 1/4$, we have $k_1 = k_2 = k_3 = k_4 \equiv K$ with $K = k_0 \exp\left[\frac{1}{4}a(U+V+W)\right]$.

Normalization allows us to eliminate one out of four equations. Performing the stability analysis, we find the eigenvalues of the following 3×3 matrix

$$\begin{aligned} \lambda_1 &= \frac{K}{2}\left[a(U+V-W)-4\right] , \\ \lambda_{2,3} &= \frac{K}{4}\left[a(U-V-W)-4 \pm \left(4+a(U-V+W)\right) i\right] . \end{aligned} \tag{4.4}$$

For $a(U+V-W) < 4$, the first eigenvalue is negative, $\lambda_1 < 0$. The real parts of $\lambda_{2,3}$ are negative for $a(U-V-W) < 4$. The complex eigenvalues $\lambda_{2,3}$ cross the imaginary axis at $a_{\text{c}} = 4/(U-V-W)$. This yields

$$\lambda_{2,3}^* = \pm i\omega(U,V,W) \,, \tag{4.5}$$

where

$$\omega(U,V,W) = 2k_0 \exp\left[\frac{U+V+W}{U-V-W}\right] \frac{U-V}{U-V-W} \,. \tag{4.6}$$

Two types of bifurcations are expected to occur in the system: pitchfork and Hopf. Their points are determined by the parameters U, V, W and a, as shown in Fig. 6. Pitchfork bifurcation occurs when the real eigenvalue λ_1 changes its sign. Similarly, the Hopf bifurcation occurs when the real parts of $\lambda_{2,3}$ change their signs. For $a > 0$, pitchfork bifurcation precedes the Hopf

bifurcation only if $V > 0$ and $0 < U - W < 4/a$. For a given parameter set (U, V, W) and for a big enough, eigenvalue λ_i with $i = 1, 2$ or 3 may change its sign. A corresponding bifurcation will then occur, affecting the dynamics of the system. This explains why the clustering of channels may lead to collective phenomena like synchronization.

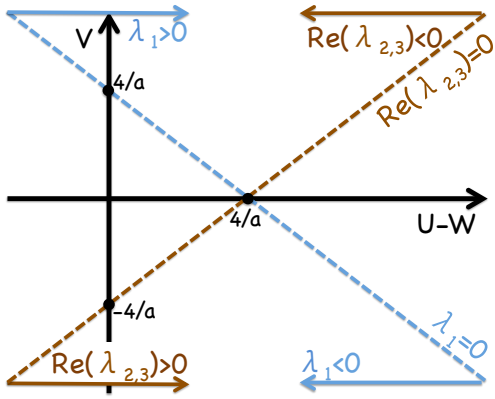

Fig. 6. (Color online) Parameter space showing the complex dynamics of a system of coupled ion channels. The light gray/blue line indicates the parameter values for which pitchfork bifurcation occurs. The dark gray/brown line sets the range for the Hopf bifurcation. See details in the text.

The choice of parameters (U, V, W) obviously determines the results obtained by modeling. It should be dictated by the biological properties of a given channel. Generally, for channels exhibiting positive cooperation (*i.e.* opening of one channel increases the opening probability of its neighbors), $U, V, W > 0$ and for those negatively coupled (*i.e.* opening of one channel decreases the opening probability of its neighbors) parameters are negative. However, combinations of positive and negative parameters are also possible and can reproduce the experimentally observed behavior.

In [9], the four-state model was suggested for nonselective voltage-activated cation channel from human red cells. By changing the membrane potential, the open channel switched to the transient-open state and eventually closed. Similarly, the closed channel was shown to open, exhibiting a transient state of "gate tension". Here, we do not introduce voltage explicitly, but by tuning the parameters, so that the equilibrium of each state is shifted towards the preceding ($|U| < |V|$) or succeeding state ($|U| > |V|$), it is possible, at least to some extent, to mimic the action of a real driving force.

Through this paper, we use $(U, V, W) = (2, -1, 0)$ as a default parameter set. This choice is justified by the physical interpretation of a channel's action under changing driving potential presented in [9]. This driving forces the channel to follow the transition cycle showed in Fig. 1 in a "positive direction" *i.e.* $1 \to 2 \to 3 \to 4$. Preceding states are then repelling (hence $V < 0$), while those ahead of the actual state are attracting ($U > 0$).

4.1. Order parameter

As a measure of the collective behavior of coupled channels, we introduce, after Kuramoto [39], synchronization order parameter r:

$$r = \frac{1}{n} \sum_{j=1}^{n} e^{i\phi_j} , \tag{4.7}$$

where ϕ_j is discrete phase of unit j. In our study we investigate 4-state units for $i = 1, 2, 3, 4$, so ϕ get simple values $\phi_i = \pi/2, \pi, 3\pi/2, 2\pi$. In this paper, we use also the notation

$$r_\infty = \langle r \rangle$$

for time that equals the last step of simulation. Parameter r_∞ characterizes phase synchrony of units.

We use the Gillespie algorithm [40] to model the stochastic transitions showed in Fig. 1 for 100 channels. Depending on the number of channels in a given state, the transition rates vary according to Eq. (4.1).

With a rise of coupling factor a, phase synchronization remains unchanged, yet until certain critical point a_c, see Fig. 7. For $a \geq a_c$ coupled units are working coherently and r is increasing rapidly. Eventually, for a big enough, r saturates at a maximum level.

5. Physiological consequences of channel synchronization

We consider an idealized cell, the membrane of which is perforated by only one type of ion channels. Each channel works in the way described in the previous section. While open (states 1 and 2), it allows the ions of a given type (*e.g.* Na^+) to flow into or outside the cell. The direction of the flow is governed by the concentration gradient g_i.

Our aim is to follow the changes of the ion concentration in such a cell, c_{in}, when channels are independent ($a = 0$ in Eq. (4.1)) and weakly ($0 < a < a_c$) or strongly coupled ($a \geq a_c$). Starting with the "empty" cell, that is with $c_{in} = 0$, we simulate the stochastic behavior of $n = 100$ channels, using the aforementioned Gillespie algorithm [40]. In each simulation step, for every channel in state 1 or 2, one molecule of ion is assumed to pass the

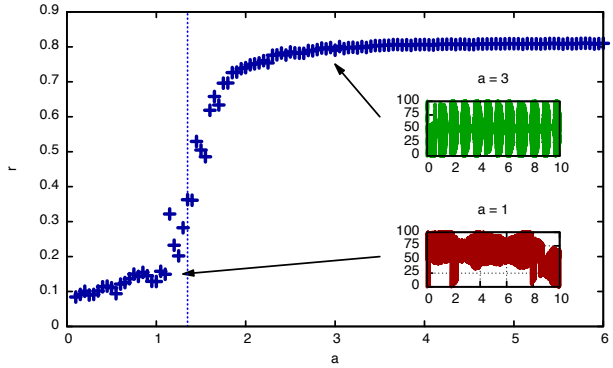

Fig. 7. (Color online) Synchronization order parameter r for $(U, V, W) = (2, -1, 0)$ and 100 oscillators. Dashed line shows the critical value of a for which $\mathrm{Re}(\lambda_{2,3}) = 0$, $a_c = \frac{4}{3}$. Simulations were done using the Gillespie algorithm, as described in the main text. Insets show the changes in the ion concentration inside the cell for sub-critical (bottom/red) and super-critical (top/green) coupling strength, a. The parameter values are $c_{\mathrm{thresh}} = 50$, $k_0 = 1$, $(U, V, W) = (2, -1, 0)$ and $n = 100$.

membrane in a direction dictated by the discrete concentration gradient, $g_i = -1, 0, 1$. For $g_i = 1$, the ions flow into the cell, while for $g_i = -1$, they flow out to the environment.

The number of molecules in the environment is assumed to be infinite. Internal concentration, c_{in}, may increase up to a threshold value c_{thresh}. For $c_{\mathrm{in}} \leq c_{\mathrm{thresh}}$, $g_i = 1$. When c_{in} exceeds the threshold, $g_i = -1$. For closed channels (states 3 and 4), no net flow is observed and $g_i = 0$.

Insets in Fig. 7 show the results of the simulations. For our choice of parameters, with growing a, eigenvalues $\lambda_{2,3}$ eventually change the sign and the Hopf bifurcation occurs. It drives the channels to cooperative action. As a result, the hypothetical ion's concentration starts to change in a regular manner. It does no longer simply fluctuate near the threshold, as for subcritical values of a (lower inset in Fig. 7). Instead, it grows and falls regularly, and the wave-like pattern resembles the electrical spikes of the changing membrane potential in excitable cells [1, 3]. Moreover, the time needed to achieve synchronization is shorter for higher values of a and the "spikes" become narrower. This behavior does not depend on the value of the threshold: when the ion concentration c_{in} approaches c_{thresh}, it starts to change in a way showed in the insets in Fig. 7. The ion's concentration is a kind of a chemical signal for the cell's metabolism. Therefore, the important result of this part is that the cell can modulate its chemical activity by allowing for or opposing the ion's clustering. We speculate that this can be done, for example, by stiffening or relaxing the membrane, *e.g.* by modifying the concentration of cholesterol in the membrane [41]. This would act as a

modulator: the signal from one channel would be transmitted to the neighboring ones easier or harder, depending on the cell's needs. This hypothesis should be tested experimentally.

6. Summary

The cooperative behavior of interacting proteins on the cell membrane is a timely and important subject of investigations [42, 43]. Local electric fields exist and arise in living cells and tissues affecting conductance of ion channels via conformational transitions within the gate area which controls transmission of ions. These conformational alterations are associated with energy barriers between states of various subconductances and are dependent on stimulus, such as electrical field or ligands. Several models have been proposed to describe the kinetics of ion channels [4]. The classical Markovian model [1] assumes that a future transition is independent of the time that the ion channel stayed in a previous state. Other models as the fractal and the chaotic [4, 44, 46] assume that the rate of transitions between the states depends on the time that the ionic channel stayed in a previous state and frequently also well conform to experimental recordings. Since the problem of identifiability of a model and discrimination between its Markov or non-Markov version is not always straightforward (some non-Markov models of kinetics, as *e.g.* proposed by the generalized Langevin equation can be well-mapped on multi-dimensional, multi-state Markov ones), Markovian approach is adopted as a first and the easiest option to test.

On the other hand, many experiments point out that biological channels behave in a cooperative manner which depends on external factors (applied voltage) or structural parameters. As an example, mechano-sensitive channels are sensitive to mechanical stimuli and adapt their conformation according to the local membrane environment. Changes of channel pore geometry in terms of electromechanical coupling between voltage sensing domains and pore-forming domains have been recently addressed by Wawrzkiewicz-Jałowiecka and Grzywna [45] in their work analyzing fluctuating permeability of the Kv 1.2 channels. These authors have pointed to the possibility of stabilization of open conformations of a channel by voltage-activation which results in the change of confinement within the pore and facilitates the transport. Neighboring channels affect themselves by membrane deformation leading to a collective response of a cluster of channels. Although these types of channels are abundant across realms of life, their behavior and self-organized cooperativity are not well-understood.

In this article, we have presented a didactic multi-state model of a single ion kinetics and explained entropy production fluxes arising in course of its opening and closing. In the second part, we have analyzed a route to a syn-

chronized behavior of an ensemble of such units coupled with their neighbors and exhibiting a transition to a collective phase motion at a critical value of the coupling parameter. We have finish with a brief resume of possible consequences of the synchronization and suggestions concerning benchmark experiments to be planned in this field.

Authors (B.L., B.D. and E.G.-N.) gratefully acknowledge financial support from the National Science Centre, Poland (NCN), grant No. DEC-2014/13/B/ST2/02014. B.L. wishes to thank the Foundation for Polish Science (International Ph.D. Projects Program co-financed by the European Regional Development Fund covering, under the agreement No. MPD/2009/6; the Jagiellonian University International Ph.D. Studies in Physics of Complex Systems) and the Jagiellonian Univeristy Institute of Physics for a donation DSC K/DSC/001586.

REFERENCES

[1] B. Hille, *Ionic Channels of Excitable Membranes*, Sinauer Associates, Sunderland, 2001.

[2] J. Walleczek, *Self-organized Biological Dynamics and Nonlinear Control*, Cambridge University Press, 2000.

[3] R. Phillips, J. Kondev, J. Theriot, *Physical Biology of the Cell*, 1st Edition, Garland Science, 2008.

[4] T. Andersson, *Math. Biosci.* **226**, 16 (2010).

[5] J. Juraszek, B. Dybiec, E. Gudowska-Nowak, *Fluct. Noise. Lett.* **5**, L259 (2005).

[6] L. Kaestner, P. Christophersen, I. Bernhardt, P. Bennekou, *Bioelectrochemistry* **52**, 117 (2000).

[7] K. Banerjee, *J. Chem. Phys.* **142**, 185101 (2015).

[8] S.M. Rappaport *et al.*, *Eur. Biophys. J.* **44**, 465 (2015).

[9] H. Flyvbjerg, E. Gudowska-Nowak, P. Christophersen, P. Bennekou, *Acta Phys. Pol. B* **43**, 2117 (2012).

[10] S.M. Bezrukov, I. Vodyanoy, *Chaos* **8**, 557 (1998).

[11] A.M. Berezhkovskii, S.M. Bezrukov, *Phys. Rev. Lett.* **100**, 038104 (2008).

[12] E. Gudowska-Nowak, B. Dybiec, H. Flyvbjerg, *SPIE Proc.* **5467**, 223 (2004).

[13] H.P. Yockey, *Information Theory, Evolution, and the Origin of Life*, Cambridge University Press, 2005.

[14] B. Das, K. Banerjee, G. Gangopadhyay, *Phys. Rev. E* **86**, 061915 (2012).

[15] H. Qian, X. Zhang, M. Qian, *Europhys. Lett.* **106**, 10002 (2014).

[16] U. Seifert, *Eur. Phys. J. B* **64**, 423 (2008).

[17] D. Hartich, A.C. Barato, U. Seifert, *J. Stat. Mech. Theor. Exp.* **2014**, P02016 (2014).
[18] K. Sekimoto, *Stochastic Energetics*, Springer Verlag, 2010.
[19] J.M. Horowitz, M. Esposito, *Phys. Rev. X* **4**, 031015 (2014).
[20] C. Van den Broeck, M. Esposito, *Phys. Rev. E* **82**, 011143 (2010).
[21] C. Van den Broeck, M. Esposito, *Phys. Rev. E* **82**, 011144 (2010).
[22] G.F. Contreras *et al.*, *Proc. Natl. Acad. Sci. USA* **109**, 18991 (2012)
[23] M. Fink, D. Noble, *Philos. Trans. A: Math. Phys. Eng. Sci.* **367**, 2161 (2009).
[24] E. Schrödinger, *What is Life*, Cambridge University Press, 1944.
[25] T. Kiss, K. Nagy, *Eur. Biophys. J.* **12**, 13 (1985).
[26] E. Yeramian, A. Trautmann, P. Claverie, *Biophys. J.* **50**, 253 (1986).
[27] O.S. Ostroumova *et al.*, *FEBS Lett.* **579**, 5675 (2005).
[28] T. Ursell, K.C. Huang, E. Peterson, R. Phillips, *PLoS Comput. Biol.* **3**, e81 (2007).
[29] K. Guseva *et al.*, *Phys. Rev. E* **83**, 020901(R) (2011).
[30] M. Sheng, E. Kim, *Curr. Opin. Neurobiol.* **6**, 602 (1996).
[31] K. Wood, C. Van den Broeck, R. Kawai, K. Lindenberg, *Phys. Rev. E* **76**, 041132 (2007).
[32] N.N. Levina, R.R. Lew, I.B. Heath, *J. Cell. Sci.* **107**, 127 (1994).
[33] M.N. Rasband, J.S. Trimmer, *Developmental Biol.* **236**, 5 (1996).
[34] J.W. Shuai, P. Jung, *Proc. Natl. Acad. Sci. USA* **100**, 506 (2002).
[35] T. O'Leary, A.H. Williams, J.S. Caplan, E. Marder, *Proc. Natl. Acad. Sci. USA* **110**, E2645 (2013).
[36] D. Bray, M.D. Levin, C.J. Morton-Firth, *Nature* **393**, 85 (1998).
[37] M.R. Kaplan *et al.*, *Neuron* **30**, 105 (2001).
[38] K. Manivannan, R.T. Mathias, E. Gudowska-Nowak, *Bull. Math. Biol.* **58**, 141 (1996).
[39] Y. Kuramoto, *Chemical Oscillations, Waves, and Turbulence*, Springer, Berlin 1984.
[40] D.T. Gillespie, *J. Phys. Chem.* **81**, 2340 (1977).
[41] J. Berg, L. Stryer, J. Tynoczko, G. Gatto, *Biochemistry*, Palgrave Macmillan, 1975.
[42] B. Lisowski, Ph.D. Thesis, Jagiellonian University, 2017.
[43] M. Bier, B. Lisowski, E. Gudowska-Nowak, *Phys. Rev. E* **93**, 012143 (2016).
[44] A. Wawrzkiewicz-Jałowiecka, B. Dworakowska, Z. Grzywna, *Biochem. Biophys. Acta* **1859**, 1805 (2017).
[45] A. Wawrzkiewicz-Jałowiecka, Z. Grzywna, *J. Chem. Phys.* **148**, 115103 (2018).
[46] A. Fuliński *et al.*, *Phys. Rev. E* **58**, 919 (1998).